

---

# Clinical Optimization of Pretargeted Radioimmunotherapy with Antibody-Streptavidin Conjugate and $^{90}\text{Y}$ -DOTA-Biotin

Hazel B. Breitz, Paul L. Weiden, Paul L. Beaumier, Donald B. Axworthy, Chris Seiler, Fu-Min Su, Scott Graves, Kyle Bryan, and John M. Reno

*Cancer Clinical Research Unit and Departments of Radiology and Medicine, Virginia Mason Medical Center, Seattle; and NeoRx Corporation, Seattle, Washington*

---

Pretargeted radioimmunotherapy (PRIT) was evaluated using an antibody-streptavidin conjugate, followed by a biotin-galactose-human serum albumin clearing agent and  $^{90}\text{Y}$ -dodecane tetraacetic acid (DOTA)-biotin as the final step for therapy. The objective was to develop a clinical protocol that could show an improved tumor-to-red marrow therapeutic ratio compared with conventional radioimmunotherapy (RIT) and at the same time preserve the efficiency of tumor targeting. **Method:** Forty-three patients with adenocarcinomas reactive to NR-LU-10 murine monoclonal antibody received the 3 components. Doses and timing parameters were varied to develop an optimized schema. In some patients, the conjugate was radiolabeled with  $^{186}\text{Re}$  as an imaging tracer to assess biodistribution of the conjugate and effectiveness of the clearing agent.  $^{111}\text{In}$ -DOTA-biotin was co-injected with  $^{90}\text{Y}$ -DOTA-biotin for quantitative imaging. Safety, biodistribution, pharmacokinetics, dosimetry, and antiglobulin formation were evaluated. **Results:** The optimal schema was defined as a conjugate dose of 125  $\mu\text{g/mL}$  plasma volume followed at 48 h by a clearing agent in a 10:1 molar ratio of clearing agent to serum conjugate. The therapeutic third step was 0.5 mg radiobiotin administered 24 h later. No significant adverse events were observed after administration of any of the components. The mean tumor-to-marrow absorbed dose ratio when using the optimized PRIT schema was 63:1, compared with a 6:1 ratio reported previously for conventional RIT. Antiglobulin to murine antibody and to streptavidin developed in most patients. **Conclusion:** This initial study confirmed that the PRIT approach is safe and feasible and achieved a higher therapeutic ratio than that achieved with conventional RIT using the same antibody.

**Key Words:** pretargeted radioimmunotherapy; NR-LU-10;  $^{90}\text{Y}$ -dodecane tetraacetic acid-biotin; monoclonal antibody

**J Nucl Med 2000; 41:131–140**

---

**P**retargeted radioimmunotherapy (PRIT) is a multistep delivery system that takes advantage of sequentially administered components to exploit antibody specificity and

applies small-molecule radioligand pharmacokinetics to increase the therapeutic ratio. Conventional radioimmunotherapy (RIT) with  $\beta$ -emitter isotopes such as  $^{131}\text{I}$ ,  $^{90}\text{Y}$ , and  $^{186}\text{Re}$  has realized only limited success in the treatment of solid tumors (1–5), in part because of slow clearance of radiolabeled antibody from circulation. The maximum tolerated dose of radioactivity that can be administered is limited to suboptimal therapeutic levels by bone marrow toxicity, the consequence of prolonged exposure to circulating radioactivity.

Several strategies have been devised to reduce the levels of circulating radiolabeled antibody. Regional administration is appropriate in specific clinical situations, e.g., ovarian cancer (6–7) or gliomas (8–9). This has had greater success than systemic RIT, because a higher therapeutic ratio can be achieved by more rapid localization of the radiolabeled antibody and lower marrow exposure. An alternative and more generally applicable approach is to reduce the amount of radioactivity in circulation after radiolabeled antibody has localized to tumor. This can be accomplished using an extracorporeal immunoadsorption column (10) or a second molecular construct, a “clearing agent,” which removes antibody from the blood (11). However, because most of the marrow radiation occurs within the first hours after administration, i.e., before removal of the radiolabeled antibody, neither of these approaches reduces the radiation exposure to marrow sufficiently to allow the administered dose to be increased as much as 2-fold.

In 1984, Goodwin first proposed a strategy to improve the tumor-to-normal organ dose ratio (12). In this strategy, the antibody serves a dual purpose, targeting the tumor and also serving as a receptor for the radioisotope. The radioisotope is administered as a later step when the tumor-to-normal organ concentration ratio is optimal. It is administered as a small molecule, rather than bound to the antibody, and thus distributes rapidly throughout the vascular and extravascular space, where it is captured by prelocalized antibody receptor in tumor. Unbound radioisotope clears quickly from circulation through renal excretion, thus reducing radiation exposure to marrow.

---

Received Nov. 30, 1998; revision accepted Jun. 21, 1999.  
For correspondence or reprints contact: Hazel B. Breitz, MD, NeoRx Corp., 410 W. Harrison, Seattle, WA 98119.

In 1987, Hnatowich et al. (13) proposed the use of avidin-conjugated antibody and radiolabeled biotin for radio-immunoscintigraphy. Avidin is a 66-kd protein found in egg white, and streptavidin (SA) is a 60-kd protein produced by *Streptomyces avidinii*. Each molecule has 4 biotin-binding sites. Biotin (vitamin H) is a 244-D bicyclic compound with a valeric acid side chain. Both avidin and SA show similar, strong biotin-binding properties. The affinity constant ( $10^{15}$  L/mol) results in rapid, highly selective, and tight binding under physiologic conditions (14).

Kalofonos et al. (15) in 1990 used antibody SA conjugate followed 2–3 d later by  $^{111}\text{In}$ -diethylenetriamine pentaacetic acid (DTPA)-biotin for imaging tumor. Squamous cell lung tumors were successfully imaged within 2 h, and background radioactivity levels were reduced in all normal tissues, including liver, kidneys, and blood.

In the pretargeted approach to RIT presented here, this approach was modified by inserting a clearing agent to improve further the tumor-to-tissue conjugate ratio. This multistep approach incorporates the following features that distinguish it from conventional RIT: the use of the antibody against tumor antigens on the tumor cell surface to carry a receptor, in this case a biotin binding receptor, rather than a cytotoxic agent; use of a clearing agent to effect removal of antibody not localized to tumor and create a differential concentration between biotin binding receptor on tumor cells and in blood that has been cleared of residual receptor; and use of the biotin binding receptor (SA) on the antibody now bound to the tumor cell surface to capture the radionuclide linked to the small molecule ( $^{90}\text{Y}$ -biotin).

Preclinical studies in tumored nude mice using this PRIT approach showed complete regressions without apparent toxicity and without regrowth in 80% of breast cancer xenografts and 100% of colon and small cell lung cancer (SCLC) xenografts (10 mice per group followed for >200 d after PRIT) (16). By comparison, using conventionally radiolabeled antibody with 7400 kBq (200  $\mu\text{Ci}$ )  $^{90}\text{Y}$  in SCLC xenografts, no cures and only a modest growth delay of 15 d was observed. Thus, in the nude mouse human tumor xenograft model, PRIT was clearly superior to RIT.

In the initial clinical study reported here, we sought to determine the feasibility of this pretargeting approach in patients and to develop a clinical protocol for therapy. The objectives of this study were to evaluate the (a) safety of the components; (b) tumor localization of NR-LU-10-SA conjugate; (c) effectiveness of the clearing agent in reducing circulating antibody conjugate; (d) pharmacokinetics of the dodecane tetraacetic acid (DOTA)-biotin; (e) ability of  $^{90}\text{Y}$ -DOTA-biotin to localize to tumor sites pretargeted with antibody-SA (using an  $^{111}\text{In}$ -DOTA-biotin tracer); (f) projected radiation absorbed dose delivered for  $^{90}\text{Y}$ -DOTA-biotin at tumor sites and in normal organs, using an  $^{111}\text{In}$ -DOTA-biotin tracer; and (g) immunogenicity of the components.

## MATERIALS AND METHODS

The 3 components assessed were monoclonal antibody (MAb)-SA chemical conjugate, clearing agent (biotin-galactose-human serum albumin [HSA]), and biotin-isotope chelate ( $^{90}\text{Y}$ -DOTA-biotin).

Three radioisotopes were used in the clinical studies:  $^{186}\text{Re}$  for radiolabeling the antibody-SA conjugate and  $^{111}\text{In}$  and  $^{90}\text{Y}$  for radiolabeling the DOTA-biotin.

### Murine MAb NR-LU-10-SA Conjugate

Murine IgG<sub>2b</sub> MAb NR-LU-10 recognizes the 40-kd epithelial antigen known as Ep-CAM, which has been studied in human clinical trials (5). NR-LU-10 (Boehringer Ingelheim, Biberach, Germany) was chemically conjugated to SA (Genzyme, Kent, UK) using succinimidyl 4-(*N*-maleimidomethyl)cyclohexane-1-carboxylate (SMCC) (Pierce, Rockford, IL) (17). NR-LU-10 was reduced with dithiothreitol, desalted by gel filtration, and mixed in 1:1 molar ratio with SMCC-SA at 5 mg/mL total protein concentration in phosphate-buffered saline (PBS). The conjugate was then purified using iminobiotin affinity chromatography and then anion exchange chromatography to remove the more highly aggregated species. The conjugate appears as a single peak on size-exclusion high-performance liquid chromatography (HPLC) with ultraviolet detection (Zorbax SEC GF250; Hewlett Packard, Wilmington, DE). By sodium dodecyl sulfate-polyacrylamide gel electrophoresis, the conjugate is about 80% 1:1 SA to antibody, with the remainder mostly 2:1 with some higher polymers. Immunoreactivity was 90% of unconjugated antibody as assessed by an enzyme-linked immunoabsorbent assay (ELISA). The biotin binding capacity (100%) was determined by 2-(4'-hydroxyphenylazo)-benzoic acid displacement from SA by biotin and by binding of radiobiotin (18). In selected patients, the conjugate was radiolabeled with 600 MBq/m<sup>2</sup>  $^{186}\text{Re}$  as previously described (5). Purity of the  $^{186}\text{Re}$ -labeled NR-LU-10-SA determined by instant thin-layer chromatography was  $\geq 90\%$ , and HPLC after the  $\gamma$  trace was  $\geq 85\%$  monomeric. Additional release assays included limulus amoebocyte assay of endotoxin burden (release criterion <5 endotoxin units/mL) (Biowittaker, Walkersville, MA), immunoreactivity evaluated by radiolabeled cell binding assay (release criterion  $\geq 45\%$ ), and biotin binding evaluated by avidin bead binding (release criterion  $\geq 90\%$ ). The stability of the  $^{186}\text{Re}$ -NR-LU-10-SA in serum was consistently >95% until the time of the DOTA-biotin injection. SDS-PAGE showed the serum to be free of metabolites or aggregates throughout the course of treatment. The conjugate biotin binding capacity in serum immediately after injection was 90% of baseline. By 24 h it was 84%, and 4 h after administration of clearing agent it was 15% ( $n = 3$ ).

### Biotin-Galactose-HSA Clearing Agent

The clearing agent was biotinylated galactose-HSA (19). The HSA was chemically derivatized with biotin through available lysine residues, and then with galactose. An average of 40 galactose residues and 2 biotins were coupled to each HSA (20). The clearing agent acted by forming complexes with the conjugate through biotin-SA interaction. It was extracted from the circulation by the Ashwell receptors of hepatocytes, which recognize its galactose sugars.

### $^{111}\text{In}$ - and $^{90}\text{Y}$ -DOTA-Biotin

The DOTA-biotin ligand, ([*N*-methyl-*N*-biotinyl]glycyl) aminobenzyl-DOTA, is made of 3 parts: amino benzyl DOTA, *N*-methyl glycine linker, and d-biotin. The *N*-methyl glycyl functions as a

linker and is designed to reduce enzymatic cleavage of DOTA biotin by serum biotinidase (17). The biotin, linked through a carboxyl group, retains functional avidin-binding activity.  $^{90}\text{Y}$  is a pure  $\beta$  emitter (Emax: 2.3 MeV) with a physical half-life of 64 h. Because  $^{90}\text{Y}$  lacks imaging photons, 185 MBq  $^{111}\text{In}$ -DOTA biotin was coadministered with 370 MBq/m $^2$   $^{90}\text{Y}$ -DOTA-biotin for tumor visualization and to evaluate biodistribution from  $\gamma$  camera imaging. In patients who received  $^{186}\text{Re}$ ,  $^{90}\text{Y}$  was not administered.  $^{90}\text{Y}$  and  $^{111}\text{In}$  are comparably stably chelated by the DOTA macrocycle (21). DTPA (100 mmol), 60 and 120  $\mu\text{L}$ , was added to chelate any free  $^{90}\text{Y}$  or  $^{111}\text{In}$ , respectively, should these be present. Preclinical studies showed that  $^{111}\text{In}$ -DOTA and  $^{90}\text{Y}$ -DOTA exhibit similar stability properties and biodistribution pharmacokinetics and are excreted unchanged in the urine (16). The release criterion of  $^{90}\text{Y}$ -DOTA-biotin by HPLC was  $\geq 90\%$  monomeric species. Gradient HPLC used a Beckman Ultraspherogel 5  $\mu\text{m}$  RPC-18 column,  $0.46 \times 25$  cm, coupled to a 170 radiodetector (Beckman, Fullerton, CA) run at 1  $\mu\text{L}/\text{min}$ . A slope gradient solvent of 0%–75% B in 15 min (5 mmol DTPA as solvent A and 1:1 ratio of 5 mmol DTPA and acetonitrile as solvent B) caused elution of free isotope at 2–3 min and labeled DOTA-biotin at 9–11 min. The purity of the labeled DOTA-biotin was 99%–100% for both  $^{111}\text{In}$  and  $^{90}\text{Y}$ . Endotoxin was  $< 5$  endotoxin units/mL. Avidin binding was assayed by avidin beads. Avidin agarose beads (Sigma, St. Louis, MO) (200  $\mu\text{L}$ ) were suspended into the top of a 0.2 microfuge (Bio-Rad, Hercules, CA) filter unit. The beads were washed twice with 200  $\mu\text{L}$  PBS, spinning the filter at 10,000 rpm. The radiolabeled DOTA-biotin in 200  $\mu\text{L}$  PBS was added to washed beads, then mixed for 5–10 min to allow binding. The radioactive beads were spun and washed twice with PBS, and bound and free radioactivity was counted in a  $\gamma$  counter. Avidin bead binding criterion was  $\geq 90\%$ , and the avidin binding was  $> 97\%$ .

### Patient Eligibility Criteria

Patients with advanced epithelial malignancies known to react by immunohistology with the NR-LU-10 antibody were eligible for study. Patients were required to have measurable or evaluable tumor refractory to standard treatment and no evidence of other serious systemic disease by history or standard measures of hepatic, renal, cardiac, and pulmonary function. Platelet count was required to exceed 100,000/mm $^3$  and white cell count to exceed 4,000/mm $^3$ . Patients were enrolled in the study only if expression of the NR-LU-10 antigen was shown by imaging with  $^{99\text{m}}\text{Tc}$ -NR-LU-10 antigen-binding fragment, Verluma (nofetumomab merpentan) (NeoRx Corp., Seattle, WA) (22,23). PRIT was performed within 1 wk of the diagnostic imaging study to avoid the possibility that human antimouse antiglobulin (HAMA) might have developed.

The study was approved by the Virginia Mason Medical Center Institutional Review Board and was conducted under an Investigational New Drug Application with the Center for Biologics Evaluation and Research, U.S. Food and Drug Administration. All patients granted informed consent after appropriate explanation of the phase I nature of this study and therapeutic alternatives.

Forty-three patients with colorectal (22), lung (10), pancreatic (3), gastroesophageal (2), bladder (2), breast (2), or ovarian (2) cancers were studied. The tumor types did not influence the dosing protocol the patients received.

### Preliminary Studies

Five patients received antibody SA conjugate (NR-LU-10-SA) only, either 40 or 200 mg, radiolabeled with  $^{186}\text{Re}$ , to assess

whether the SA altered the pharmacokinetics, biodistribution, and tumor targeting of the antibody.  $^{186}\text{Re}$  was used as the radiolabel because of our experience with  $^{186}\text{Re}$ -NR-LU-10 (5).

Two patients each received 2 mg  $^{111}\text{In}$ -DOTA-biotin alone to study the biodistribution of the radioligand.

### Pharmacokinetics

Serum was collected at 0.2, 1, 24, and 48 h after injection of conjugate, and at 0.2, 1, 2, 4, 6, 8, 12, and 24 h after injection of the clearing agent. When conjugate was not radiolabeled, conjugate clearance was assessed by ELISA and, when radiolabeled, by  $^{186}\text{Re}$  counting in a  $\gamma$  counter. Serum and urine were counted after the administration of DOTA-biotin to compare the pharmacokinetics of the  $^{111}\text{In}$ - and  $^{90}\text{Y}$ -DOTA-biotin. Serum was counted at 0.2, 1, 2, 4, 6, 8, 12, 24, 48, and 116 h. Urine was collected only in a limited number of patients, because of radiation exposure concerns for medical personnel. Thus, we relied on whole-body counting by  $\gamma$  camera to assess whole-body clearance. Samples were counted in a  $\gamma$  counter for  $^{111}\text{In}$  and a liquid scintillation counter for  $^{90}\text{Y}$  (24). Serum data were fit to a 2-compartment model with bolus input and first-order output. The elimination half-life was calculated using PKAnalyst (Micromath Scientific Software, Salt Lake City, UT). Fast-performance liquid chromatography analysis was performed on the serum of 6 patients to assess the contribution of the free DOTA-biotin and conjugate-bound DOTA-biotin. After an acceptable schema was developed, an escalation study of the  $^{90}\text{Y}$  dose was initiated and will be reported separately. To increase the sample size of the pharmacokinetic data reported here, we have included 15 patients from the dose escalation study who received the components of the optimized schema described below.

### Dosimetry

Biodistribution of  $^{111}\text{In}$  DOTA-biotin in organs and tumor was evaluated by quantitative planar  $\gamma$  camera imaging using a Maxxus camera with a medium-energy collimator and a 400i computer (General Electric Medical Systems, Milwaukee, WI). Radiation absorbed dose to evaluable tumors and organs was estimated using standard MIRD techniques (25–29) and will be reported in detail separately. Images were acquired from both the 173- and 247-keV photopeaks.  $^{90}\text{Y}$  dosimetry was modeled from the  $^{111}\text{In}$  data.

Attenuation correction for conjugate view data was based on  $^{57}\text{Co}$  flood source transmission, corrected for  $^{111}\text{In}$ . The correction was based on patient studies with both isotopes. For single-view source organs, attenuation correction was based on depth derived from CT scans. Whole-body-counting and planar spot images were acquired immediately and at 3, 20, 44, and 115 h after injection. Regions of interest (ROI) were drawn over the source organs, with a background ROI close to the source organ. These included the thyroid gland, kidneys, liver, bladder, entire intestinal tract, and tumors. Activity observed in the gastrointestinal tract was assumed to be related to localization on the antigen expressed in normal intestinal mucosa, consistent with histopathologic assessment of intestinal antigen expression. Because the small intestine accounts for two thirds of the total intestinal mass, the intestinal dose was estimated by assigning two thirds of the intestinal activity from the abdominal ROI to the small intestine and using the MIRD model for the intestinal tract to estimate the dose to the small-intestine wall (29). Residence times were determined for the source organs by trapezoidal integration of time-activity curves with exponential fitting to determine long-term retention.

Dose to the bone marrow was estimated from circulating radioactivity. The radiolabel was assumed to bind immediately to

the conjugate. The conventional approach for marrow dose from radiolabeled antibodies was used, assuming the concentration of activity in marrow to be 0.25 relative to that of the blood (30). Residence times were calculated from the  $^{111}\text{In}$  and  $^{90}\text{Y}$  counted in the serum.

The absorbed dose to the patient was adjusted for actual patient mass. The absorbed dose to the liver was adjusted for liver mass when hepatic metastases were present (28). MIRD phantom organ masses were used for the other organs. Tumor dose was estimated when tumor was visible on the images and tumor mass could be derived from cumulative areas on CT slices. Tumors were modeled as for organs and adjusted for mass (28). S-factors from the International Commission on Radiation Protection and Measurement, as implemented in MIRDOSE2 software (RIDIC, Oak Ridge, TN), were used to estimate the radiation absorbed dose.

## Safety

Patients were monitored for toxicity by periodic evaluation of symptoms and signs and by clinical laboratory analyses. Standard toxicity and tumor response criteria were used (31).

Patients were monitored for the production of HAMA, antistreptavidin antibody (HASA), and anticonjugate antibody (HACA). Antiglobulin levels were measured in patient sera using a sandwich-based ELISA in a format previously described (5). Briefly, streptavidin, NR-LU-10, or NR-LU-10/SA were used as capture antigens for HASA, HAMA, and HACA, respectively. In each case, antigen was coated overnight at  $4^\circ$  on 96-well polyvinyl microliter plates (Falcon Plastics, Oxnard, CA) in PBS at  $1\text{ }\mu\text{g/mL}$ . Patient sera were added for 1 h at room temperature in 4-fold dilutions to wells in PBS containing 0.5% Tween (Sigma Chemicals, St. Louis, MO) and 4% chicken serum (Sigma) (PBS chicken serum Tween buffer). After washing unbound sera components, peroxidase-labeled goat antihuman (H and L chain) antibody was added in PCT for each of the 3 assays for 45 min. After additional washes, the chromogen substrate, 2,2'-azino-bis-3-ethylbenzothiazoline-6-sulfonic acid (0.28 mg/mL) was added, and color development was monitored spectrophotometrically at 45 nm.

Relative reactivity was determined by measuring the HASA, HAMA, and HACA immune response relative to a pooled serum source of untreated normal individuals for the purpose of standardizing the immune response among different patients (5). To be considered a positive HAMA response, post-treatment levels needed to be at least 2 times higher than pretreatment levels. Using these techniques, qualitative assessments in the patient response to the various components could be made.

## RESULTS

### Preliminary Studies

The mean serum clearance of  $^{186}\text{Re}$  NR-LU-10-SA conjugate from the 5 patients who received 40 ( $n = 2$ ) or 200 ( $n = 3$ ) mg is shown in Figure 1. For comparison, serum clearance of 40 mg  $^{186}\text{Re}$ -NR-LU-10 antibody alone ( $n = 15$ ) is shown. The elimination half-time of NR-LU-10-SA

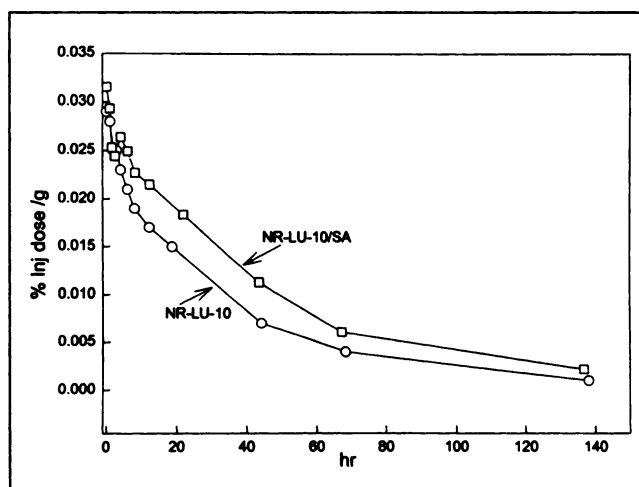


**FIGURE 1.** Mean serum clearance of  $^{186}\text{Re}$ -NR-LU-10 antibody ( $n = 15$ ) and  $^{186}\text{Re}$ -NR-LU-10-SA conjugate ( $n = 5$ ).

was 27.2 h compared with 21.6 h for antibody, a statistically significant difference ( $P < 0.001$ ). While these clearance curves are statistically different, likely as a result of the altered charge and increased size of the molecule, a difference of this magnitude seemed unlikely to be of clinical significance. More important,  $\gamma$  camera imaging showed that tumor targeting and organ biodistribution of the SA conjugate were comparable with those of unconjugated NR-LU-10.

Two patients received  $^{111}\text{In}$ -DOTA-biotin alone. The radio-ligand was primarily excreted in the urine. Images showed no retention in the organs, no nonspecific tumor localization, and minimal hepatobiliary excretion (32). Because of the rapid extravasation of the radiobiotin from the circulation, at 10 min after administration only 19% of the injected dose (ID) remained in the serum, and by 8 h  $<1\%$  remained. The first-order serum elimination half-time was 1.2 h. By 24 h, 97% of the ID had been excreted intact in the urine. No free radioisotope was detected in urine. Dosimetry estimates projected for  $^{90}\text{Y}$ -DOTA-biotin alone were bladder, 3.0 mGy/MBq (11 rad/mCi); whole body, 0.035 mGy/MBq (0.13 rad/mCi); kidneys, 0.35 mGy/MBq (1.3 rad/mCi); liver, 0.03 mGy/MBq (0.11 rad/mCi); bone marrow, 0.012 mGy/MBq (0.047 rad/mCi); and thyroid, 0.032 mGy/MBq (0.12 rad/mCi).

### Component Dosing Optimization

Initially, several patients were dosed on the basis of results from preclinical animal studies, but dosing and timing adjustments were required to improve the biodistribution in patients. The range of doses and timing intervals were as follows:

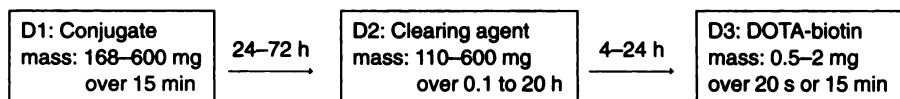


**TABLE 1**  
Dosing and Timing Parameters

Patient no.	D1 (mg)	T1 (h)	D2 (mg)	T2 (h)	D3 (mg)
1	170	24	110	4	0.5
2	200	24	150	4	0.5
3	200	24	300	4	0.5
4	200	44	300	4	0.5
5	400	44	300	10	0.5
6	400	46	300	24	2
7	200	48	300	24	2
9	200	48	300	24	2
10*	200	48	300	24	2
12	400	48	400	24	2
14	400	48	400	24	0.5
15	600	48	600	24	2
18	400†	48	400	24	0.5
19	400	48	350	24	0.5
20	400	48	400	24	0.5
21	400	48	400	24	1.5
22	400	48/58	350/50	24	0.5
23	401	48/59	350/51	24	1.5
25	400	48	400	24	0.5
29	400	48	400	24	0.5
30	400	48/58	350/50	24	0.5
31	400	48	400	24	0.5
32	300	48	400	24	0.5
33	300	48	400	24	0.5
35	400	72	400	24	0.5
36	400	72	400	24	0.5
37	400	48/62	200/200	10/34	0.5/0.5
38	200	48	350	24	0.5
39	250	48	260	24	0.5
41	300	48	360	24	0.5
42	360	48	315	24	0.5
43	345	48	415	24	0.5
44	262	48	500	24	0.5
46	336	48	220	24	0.5
47	410	48	230	24	0.5
49	442	48	450	24	0.5
50	380	48	400	24	0.5
51	300	48	312	24	0.5
54	425	48	440	24	0.5
57	298	48	301	24	0.5

\*Patients 11, 13, 16, and 17 received increasing doses of  $^{90}\text{Y}$ .

†Patient 18 received 276 mg unconjugated antibody 72 h before conjugate.

D1 = conjugate mass dose; D2 = clearing agent mass dose; D3 = dodecane tetraacetic acid-biotin mass dose; T1 = interval from D1 to D2; T2 = interval from D2 to D3.

Table 1 shows the doses and timing intervals of the components for all 43 patients. Numbers not listed represent patients who did not receive the complete protocol because of failure to image tumor with  $^{99\text{m}}\text{Tc}$ -Fab-NR-LU-10, planned surgical resection after conjugate administration, progressive disease, etc. Not all combinations of doses and timing could be evaluated, and decisions to change parameters were frequently made after evaluation of data from just 1 or 2 patients. Data evaluated included qualitative assessment of planar imaging and quantitative evaluation of blood, urine,

and whole-body clearance kinetics and radiation absorbed dose estimates to organs. Thus, parameter changes were based on evaluating available preclinical and patient data. Although more detailed study of the parameters and larger patient numbers would have been preferable, limited resources confined us to this approach.

Preliminary observations were that (a) administration of the individual components in a combined protocol was safe; (b) conjugate was effectively removed from circulation by the clearing agent to the liver, where it was metabolized and excreted into the gut (as indicated by the  $^{186}\text{Re}$  radiolabel); and (c) radiobiotin rapidly localized to pretargeted conjugate. The overall objective of these studies was to maximize the projected radiation dose to tumor while maintaining a high tumor-to-bone marrow dose ratio.

**D1 (NR-LU-10/SA).** Conjugate was administered as an intravenous infusion over 15 min in each patient. High doses were given to achieve the highest intravascular concentrations that could still be cleared effectively from the body. The aim was to saturate available tumor antigen sites with conjugate and achieve uniform distribution of SA throughout the tumor, although this was not directly evaluated. Tumor uptake had to be considered in conjunction with uptake in normal organs that express the antigen. The kidneys and gastrointestinal tract, known to express the antigen (5), were of particular concern, because images and dosimetry estimates indicated that localization of the  $^{90}\text{Y}$  could be potentially harmful at high dosages. In patient 15, 600 mg conjugate were given and high kidney uptake was noted. This was assumed to be related to the antigenic expression by the kidney, so conjugate dose was reduced. Patient 18 received 276 mg antibody 72 h before conjugate in an attempt to preferentially block kidney uptake, but tumor uptake appeared to be similarly reduced. Several antibody lots and native and recombinant SA were studied for consistency. The optimal dose was determined to be 400 mg. However, to achieve more patient-to-patient consistency, dosing was modified on the basis of estimated plasma volume. A mass dose of 125  $\mu\text{g}$  conjugate per milliliter of plasma volume, which approximates a 400-mg patient dose, was adopted and used from patient 38 onward.

**T1 (Timing Interval Between Conjugate and Clearing Agent Administrations).** Because conjugate pharmacokinetics are relatively slow, a sufficient interval is needed for peak uptake in tumor. Preclinical and clinical studies with  $^{186}\text{Re}$ -NR-LU-10 showed peak uptake in tumor at 24–48 h after infusion (5). We tested 24 h, 44–48 h, and 72 h as T1 (see Table 1). Because of the possibility of biotin filling of the tumor over time and therefore reduced biotin binding capacity for the DOTA-biotin, and because conjugate tumor localization was similar to antibody, 48 h was selected as optimal.

**D2 (HSA Clearing Agent).** There was no obvious difference in the effectiveness of clearing agent, whether given by intravenous bolus or continuous infusion over a 24-h period or split into 2 equal doses given at various times over 24 h.

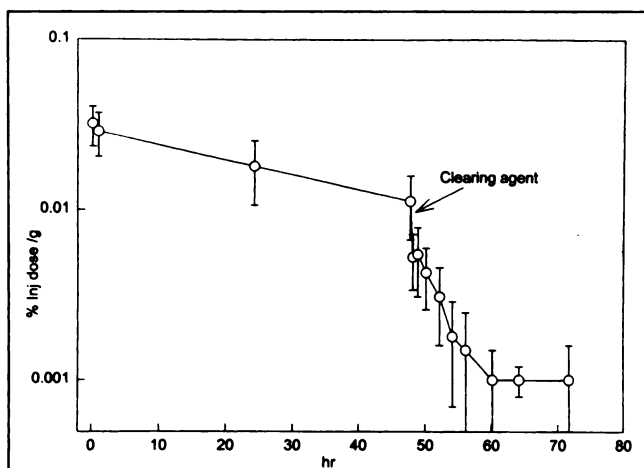


**FIGURE 2.** NR-LU-10-SA conjugate serum concentration determined by ELISA ( $n = 22$ ). At 48 h after conjugate administration, clearing agent was administered. DOTA-biotin was injected at 72 h.

Bolus injection was most simple and was used from patient 38 onward. The doses evaluated ranged from 110 to 600 mg. The dose of clearing agent as its molar ratio to the amount of conjugate remaining in blood at the time of administration was calculated, and various molar ratios were evaluated. As assessed by imaging and blood clearance kinetics, the best performance consistency was achieved when this ratio was 10:1, approximating a dose of 350–400 mg. Higher doses of clearing agent compromised the uptake of subsequently administered radio-DOTA-biotin.

The serum clearance pharmacokinetics of conjugate before and after clearing agent administration for 22 patients on the optimized protocol receiving 125  $\mu\text{g/mL}$  plasma volume and a 10:1 molar ratio of clearing agent is shown in Figure 2. This was equivalent to  $\sim 400$  mg conjugate and  $\sim 400$  mg clearing agent. At the time of administration of the clearing agent (48 h) 40% of the ID of conjugate remained in the serum. Between 48 and 60 h, mean conjugate levels in serum dropped from  $0.0113 \pm 0.0046$  to  $0.001 \pm 0.0005$  %ID/g, a 93% reduction. The formation of complex is apparently immediate, but there is a limited capacity of the liver to process the complex; thus, 12 h are required before the nadir of the conjugate in the serum occurs. Images of  $^{186}\text{Re}$ -labeled conjugate (Fig. 3) illustrate the extraction of

conjugate from blood pool into the liver and subsequent metabolism and excretion into gut.

**T2 (Time Interval Between Clearing Agent and Radio-DOTA-Biotin).** Initially, radiobiotin was administered 4 h after clearing agent. This resulted in relatively high liver uptake of the radioligand, i.e.,  $\sim 12\%$  of the ID. This may have been due to conjugate-clearing agent complex cleared to the liver but not yet completely metabolized and thus still available to bind  $^{111}\text{In}$ -DOTA-biotin on hepatocyte cell surfaces. Increasing the interval to 10 h or more resulted in significantly less liver uptake. When the interval was 24 h,  $\sim 3\%$  of the ID localized to the liver, consistent with this hypothesis. Therefore, 24 h was selected as optimal.

**D3 (Mass Dose of DOTA-Biotin).** Most patients received 0.5 mg or 2 mg of DOTA-biotin (Table 1). In patients who received the 2-mg dose, lower radiation absorbed doses were estimated in tumor compared with patients given the 0.5-mg dose. A bolus administration of 0.5 mg was found to be equally as effective as a 15-min infusion and was therefore adopted.

The serum clearance of 0.5 mg pretargeted  $^{111}\text{In}$ -DOTA-biotin ( $n = 22$ ) is shown in Figure 4A. The serum clearance of nonpretargeted  $^{111}\text{In}$ -DOTA-biotin ( $n = 2$ ) is included for comparison. The serum clearance was biexponential; with a mean  $\alpha$  half-time of 0.4 h and a  $\beta$  clearance half-time of 33 h, the first-order plasma elimination constant was 10.3 h. At 2 h, 10% of the ID remained in circulation. FPLC analysis showed that by 6 h, all of the radiobiotin remaining in serum was bound to conjugate. The rapid urinary excretion of free radiobiotin resulted in decreased blood pool background at early time points. Whole-body counting indicated that  $36\% \pm 8\%$  of the injected radioactivity had been excreted by 2.5 h and  $65\% \pm 3\%$  had been excreted by 21 h. Urinary analysis confirmed excretion of intact radiobiotin, with no change in HPLC retention and immobilized avidin binding activity (24) relative to the injected material. The serum clearance of  $^{90}\text{Y}$ -biotin was similar to that of  $^{111}\text{In}$ -biotin (Fig. 4B).

After administration of the radiobiotin, there was rapid localization of radiolabel to tumor within minutes of administration (Fig. 5). The radiolabel remained in tumor through the last imaging time point at 115 h (Fig. 6). Abdominal images from another patient at 3 h after  $^{111}\text{In}$ -DOTA-biotin showed prominent activity in the kidneys and the gastrointes-

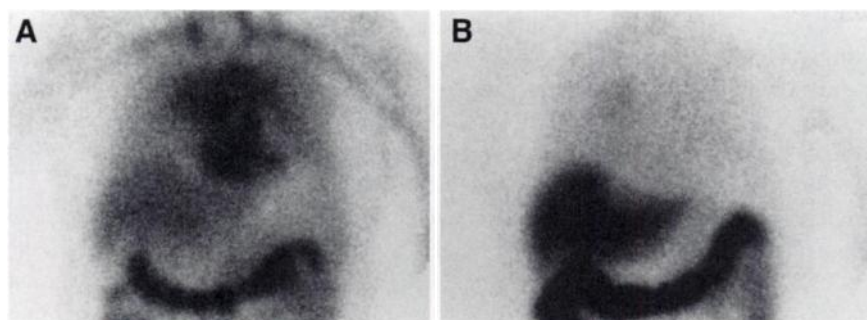


**FIGURE 3.**  $^{186}\text{Re}$ -labeled NR-LU-10-SA conjugate anterior chest images. (A) Forty-six-hour image, before clearing agent administration. (B) Twenty-three hours after clearing agent, before DOTA-biotin administration.



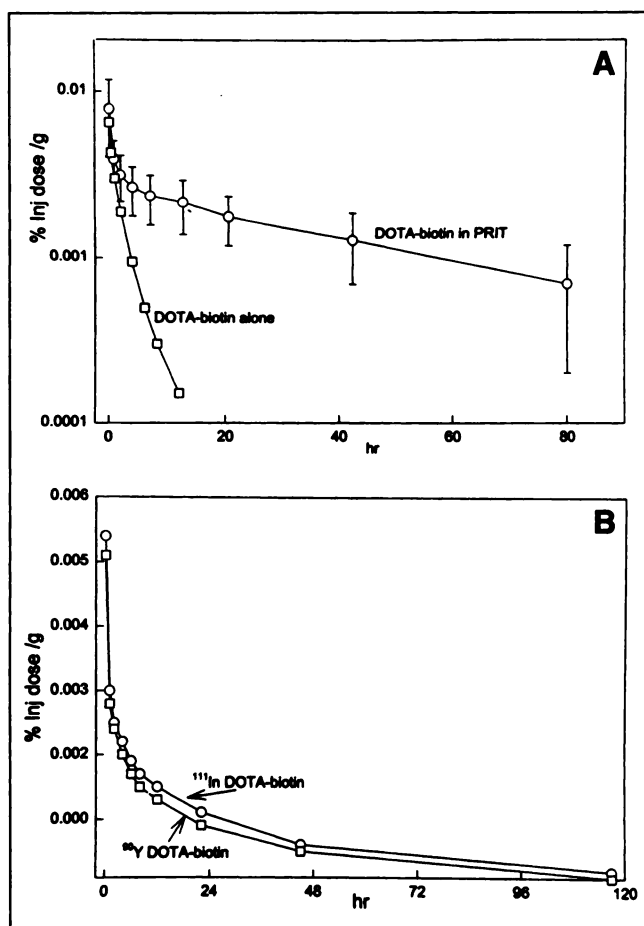


**FIGURE 4.** (A) Serum clearance of  $^{111}\text{In}$ -DOTA-biotin alone ( $n = 2$ ) versus serum clearance of  $^{111}\text{In}$ -DOTA-biotin in optimal PRIT schema ( $n = 22$ ). (B) Comparison of  $^{111}\text{In}$ - and  $^{90}\text{Y}$ -DOTA-biotin serum clearance in patient.

tinal tract (Fig. 7). This is because of the cross-reactivity of the antibody with antigen expressed in the collecting tubules of the kidneys and in the mucosa of the intestinal tract.

**Optimal Schema.** In summary, the optimal schema was a conjugate dose of 125  $\mu\text{g/mL}$  plasma volume, followed by clearing agent dosed as a 10:1 molar ratio at 48 h, and 24 h later by 0.5 mg DOTA-biotin. This was similar to the preclinical study but with longer time intervals because of the lower metabolic rate of patients compared with mice.

### Dosimetry

Radiation absorbed dose estimates (Table 2) are reported for patients receiving 0.5 mg DOTA-biotin ( $n = 34$ ) from

the quantitative imaging data. The doses to the gastrointestinal tract underestimate the true dose, because the standard MIRD model assumes all activity to be in the luminal contents. In 29 patients who had marrow dosimetry estimates from both  $^{111}\text{In}$  and  $^{90}\text{Y}$ , the mean red marrow projected dose from  $^{111}\text{In}$  was 0.089 mGy/MBq (0.33 rad/mCi), similar to that from directly counting  $^{90}\text{Y}$  in the serum, 0.073 mGy/MBq (0.27 rad/mCi). Preclinical studies with this chelate indicate that there is no localization of  $^{90}\text{Y}$  in the bone. This was not evaluated by biopsy in patients; thus, it is possible that the  $^{90}\text{Y}$  did localize in bone and that the doses were underestimated. Of these calculated marrow doses, less than 7% was contributed by free radio-DOTA-biotin. In 9 patients who received the optimized protocol, the average dose estimated to tumor was 5.4 mGy/MBq (20 rad/mCi), with 10.8 mGy/MBq (40 rad/mCi) being the highest. Mean tumor-to-marrow dose ratio in this group was 63:1.

### Toxicity and Response

No gradeable hematologic toxicities were reported for any patient on the optimization protocols, even though patients received 370 MBq/ $\text{m}^2$   $^{90}\text{Y}$ . Nonhematologic toxicities possibly related to the study components included minor (grade I) elevations in liver function tests, (lactate dehydrogenase [9], serum glutamic-oxaloacetic transaminase [SGOT, 6], alkaline phosphate [5], serum glutamic-pyruvic transaminase [3], bilirubin [1]), fatigue (8), fever (6), nausea (4), anorexia (1), diarrhea (1), abdominal pain (1), elevated thyrotropin (1), proteinuria (1), and elevated serum urea nitrogen (1). One patient had a grade II SGOT elevation. No tumor responses were observed at these doses.

**Human Antibody Response.** The immune response to the murine antibody, SA, and the antibody-SA conjugate in 17 patients is compiled in Table 3. Data are presented as the geometric mean in normal human serum units. Three patients received 200 mg conjugate and no clearing agent. Seven patients received 200 mg conjugate followed by 300 mg clearing agent 48 h later. Seven patients received 400 mg conjugate followed by 400 mg clearing agent 48 h later.

In most patients, HAMA, HASA, and HACA developed by the second week after therapy. There is no evidence, based on the few patients evaluated who did not receive clearing agent, that the clearing agent substantially altered levels of HAMA, HASA, or HACA.

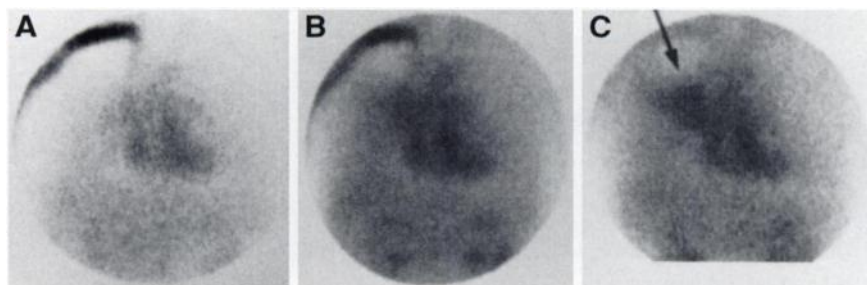
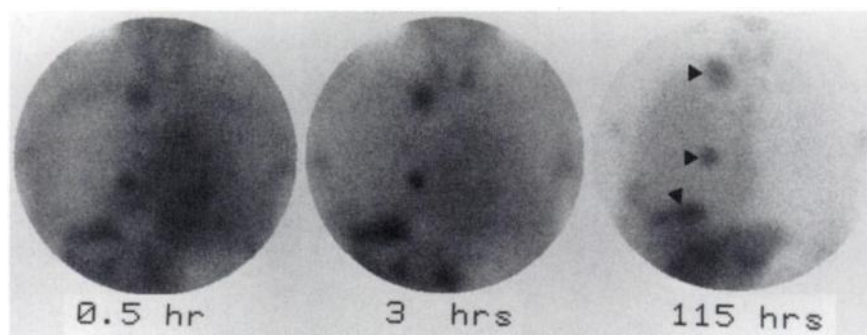


**FIGURE 5.**  $^{111}\text{In}$ -DOTA-biotin was administered as 15-min infusion in patient 4, who had carcinoma of right lung (arrow). Serial 1 min anterior chest images were acquired. Images shown are at 2 (A), 9 (B), and 16 min (C) after injection and show rapid tumor uptake of DOTA-biotin.

**FIGURE 6.** Anterior chest images in patient 14, with rectal cancer and metastases to liver and pleura-based nodules in right chest. Nodules were seen immediately after injection and through 115 h imaging time.



## DISCUSSION

Although the use of an antibody as a targeting vehicle has long been considered an attractive approach for the treatment of cancer, intact MABs are not ideal carriers of radiation, because of the relatively long time required for antibody to localize in tumor and clear from the circulation. In the pretargeted approach, the role of the antibody has been modified from a carrier of the therapeutic isotope to the carrier of a receptor for the therapeutic isotope, while still taking advantage of the antigen specificity.

The initial pretargeting method studied used a bispecific antibody (33). Bispecific antibodies are engineered with tumor antigen specificity on 1 arm and specificity for a small radiolabeled hapten ion on the other arm. Tumor-to-nontumor uptake ratios were improved, but because of the monovalency, absolute tumor targeting was reduced (33). The use of bivalent haptens increased the tumor localization to the bispecific antibodies (34). A study with anticarcinoembryonic antigen (antiCEA)-anti-In-DTPA bispecific antibody in 11 patients reported the influence of different doses and time intervals on this 2-step approach but did not define an optimal protocol (35). Important findings included improved tumor-to-nontumor localization of radioactivity in tumor and comparable absolute tumor localization when compared with the directly labeled  $F(ab')_2$  antibody. The pharmacokinetics were comparable with the SA-biotin approach in our studies. Pretargeting with bispecific antibodies is being evaluated for therapy of patients with SCLC and medullary thyroid cancer using this bispecific antiCEA antibody and  $^{131}I$  bivalent hapten. Doses of 20–80 mg antibody are infused, and 4 d later up to 160 mCi  $^{131}I$  are administered to the patients with SCLC. At this dose level,

harvested peripheral blood stem cells were reinfused. (36). In the patients with medullary thyroid cancer, 45 mCi/m<sup>2</sup> was the maximum tolerated dose. Although tumor-to-nontumor ratios were improved, hematologic toxicity was dose limiting at similar dose levels to that of radiolabeled antibody RIT (37).

Paganelli et al. (38) investigated pretargeted biotinylated antibodies for both imaging and therapy. Biotinylated antibody was followed 1–5 d later by 2 injections of avidin. In this scheme, avidin functioned as a clearing agent to remove circulating biotinylated antibody and at the same time localized to biotinylated antibody on the tumor cells and functioned there as the radiobiotin receptor. Radiolabeled biotin was administered 48 h later. Using an antiCEA  $F(ab')_2$  fragment, Paganelli et al. detected tumors within 3 h of administration of  $^{111}In$ -biotin in all 18 patients studied. Urinary excretion was more rapid using this approach, 63%  $\pm$  5% excreted within 3 h, but localization in liver, kidneys, and tumor was similar to that in our study. Paganelli et al. also used pretargeted biotinylated antitenascin antibody HC4 to treat patients with glioma. Biotinylated antibody, 35 mg/m<sup>2</sup>, was followed 36 h later by 30 mg avidin and 50 mg SA, and then 18–24 h later by 1–2 mg  $^{90}Y$ -DOTA-biotin. Optimization of these components for therapy has not been reported, but this approach has been successful in achieving clinical responses in patients receiving 2.96 GBq/m<sup>2</sup>  $^{90}Y$  without dose-limiting myelosuppression (39).

Our pretargeting schema modified the original approach described by Kalofonos et al. (15) by inserting a clearing step to improve the therapeutic ratio. Preclinical studies in the murine model showed increased therapeutic efficacy of

**FIGURE 7.** Anterior (A) and posterior (B) abdomen images from patient 50 at 3 h. Prominent  $^{111}In$ -DOTA-biotin activity was present in bladder from excretion and in gastrointestinal tract and kidney because of localization at antigenic sites expressed in epithelial cells of these organs. Note minimal activity in liver.

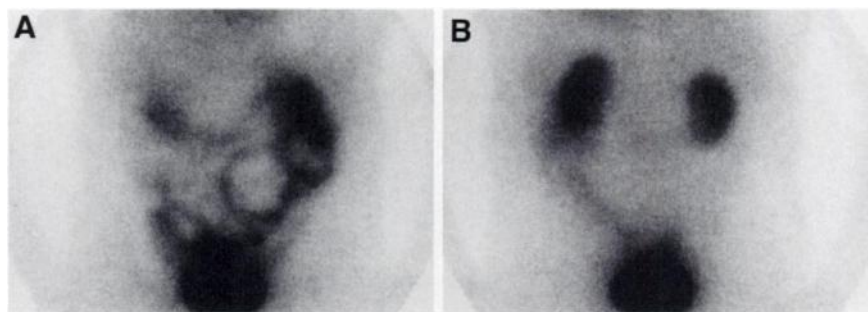




**TABLE 2**  
PRIT Radiation Absorbed Dose from Patients Receiving  
0.5 mg DOTA-Biotin

	mGy/MBq <sup>90</sup> Y Mean ± SD	mGy/MBq <sup>90</sup> Y Range	Rad/mCi <sup>90</sup> Y Mean ± SD
Tumor	3.4 ± 2.5	0.27–10.7	12.7 ± 9.5
GI tract	2.6 ± 1.1	0.74–4.9	9.9 ± 4.2
Kidneys	3.5 ± 1.7	1.0–7.6	13.3 ± 6.2
Liver	1.0 ± 0.03	0.35–1.7	3.6 ± 0.1
Thyroid	0.8 ± 0.6	0.05–2.1	3.1 ± 2.1
Whole body	0.2 ± 0.08	0.1–0.45	0.8 ± 0.3
Marrow	0.10 ± 0.06	0.02–0.32	0.37 ± 0.21

From <sup>111</sup>In data as described in text, n = 34.

this PRIT schema compared with conventional RIT (5) and led us to perform this phase I study to optimize a PRIT protocol for patients. Comparison of the serum pharmacokinetics from this phase I study with those from conventional RIT are encouraging. The lower circulating radioactivity combined with the immediate uptake of the therapeutic radionuclide using the PRIT approach resulted in an improved tumor-to-marrow dose ratio compared with conventionally labeled NR-LU-10, i.e., 63:1 for PRIT (n = 9) compared with 6:1 for conventional RIT (5).

Using the components described, the tumor-to-marrow dose ratios suggest that the total <sup>90</sup>Y activity administered can be substantially increased. The absorbed dose estimates to tumor per unit administered activity did not increase as was anticipated by the presence of the 4 biotin binding sites to capture the radioisotope. Though accurate tumor dosimetry is difficult to obtain, our experience and dose estimates suggest that tumor uptake was highly variable. Immunohistologic analysis of tumor biopsies obtained from patients between 48 and 72 h after conjugate administration suggest

that over time, biotin binding capacity of prelocalized antibody SA was reduced by filling with endogenous biotin. Because levels of circulating endogenous biotin are low, we hypothesize that biotin released from the liver into circulation after clearance and processing of biotinylated clearing agent is responsible for this effect.

This suggests that 1 way to improve the PRIT system would be to develop a clearing agent with a metabolically stable biotin linkage. A second generation, redesigned clearing agent is now being evaluated.

The application of the clearing agent is of obvious benefit in reducing nontarget radiation burden. However, the clearing agent only removes circulating conjugate and does not alter conjugate distribution to antigen positive tissues, which is dictated by the specificity of the antibody. Thus, another limitation of the study described here was cross-reactivity of the pan-carcinoma NR-LU-10 antibody with normal tissues, particularly the kidney and gut. We are therefore exploring alternative antibodies with greater specificity and less cross-reactivity as candidates for PRIT.

## CONCLUSION

We have shown that this 3-component (conjugate, clearing agent, radiobiotin) PRIT system is feasible and safe. A significant improvement in the therapeutic ratio has been shown with PRIT relative to conventionally labeled MAb RIT. This should allow a higher total amount of <sup>90</sup>Y activity to be administered, thus increasing the total radiation absorbed dose to tumor. An optimized dose and timing schema was identified using the current components, and we have initiated a dose escalation study to define the maximum tolerated dose, first organ of toxicity, and dose-limiting toxicity (40).

**TABLE 3**  
Antiglobulin Levels After PRIT

	Baseline			Week 2			Week 4		
	HASA	HAMA	HACA	HASA	HAMA	HACA	HASA	HAMA	HACA
200 mg conjugate									
Geometric mean	1	1	2	ND	ND	ND	362	111	307
Range	1–5	1–3	1–3	ND	ND	ND	120–1098	70–176	129–731
200 mg conjugate + 300 mg clearing agent									
Geometric mean	NA	NA	NA	3	4	9	39	28	173
Range	0–4	0–8	0–9	0–396	1–90	2–351	2–2408	3–146	7–1602
400 mg conjugate + 400 mg clearing agent									
Geometric mean	NA	NA	NA	3	30	22	190	102	343
Range	0–2	0–1	0–2	0–61	1–263	2–376	32–1529	48–276	90–581

Two to eight patient samples were evaluated at each data point.  
ND = no data; NA = not available.

## ACKNOWLEDGMENTS

The authors thank Janet Appelbaum, Becky Bottino, Mark Hylarides, Bob Mallett, and Lou Theodore at NeoRx Corp., Seattle, WA; Sonia Kunz and Barbara Ratliff at Virginia Mason Medical Center, Seattle, WA; and Darrell Fisher at Pacific National Northwest Laboratories, Richland, WA, for their contributions to this project. This work was supported by NeoRx Corp., Seattle, WA.

## REFERENCES

1. Tempero M, Lechner P, Dalrymple G, et al. High-dose therapy with iodine-131-labeled monoclonal antibody CC49 in patients with gastrointestinal cancers: a phase I trial. *J Clin Oncol*. 1997;15:1518-1528.
2. Meredith RF, Bueschen AJ, Khazaeli MB, et al. Treatment of metastatic prostate carcinoma with radiolabeled antibody CC49. *J Nucl Med*. 1994;35:1017-1022.
3. Press OW, Eary JF, Appelbaum FR, Bernstein ID. Radiolabeled antibody therapy of lymphomas. In: DeVita VT, Hellman S, Rosenberg SA, eds. *Biologic Therapy of Cancer*. Vol. 4. Philadelphia, PA: Lippincott; 1994:1-13.
4. Behr TM, Sharkey RM, Juweid ME, et al. Phase I/II clinical radioimmunotherapy with an iodine-131-labeled anti-carcinoembryonic antigen murine monoclonal antibody IgG. *J Nucl Med*. 1997;38:858-870.
5. Breitz HB, Weiden PL, Vanderheyden J-L, et al. Clinical experience with Re-186-labeled monoclonal antibodies for radioimmunotherapy: results of phase I trials. *J Nucl Med*. 1992;33:1099-1112.
6. Hird V, Stewart JSW, Snook D, et al. Intraperitoneally administered <sup>90</sup>Y-labeled monoclonal antibodies as a third line of treatment in ovarian cancer: a phase 1-2 trial—problems encountered and possible solutions. *Br J Cancer*. 1990;10:48-51.
7. Jacobs AJ, Fer M, Su F-M, et al. A phase I trial of a rhenium-186-labeled monoclonal antibody administered intraperitoneally in ovarian carcinoma: toxicity and clinical response. *Obstet Gynecol*. 1993;82:586-593.
8. Riva P, Arista A, Franceschi G, et al. Local treatment of malignant gliomas by direct infusion of specific monoclonal antibodies labeled with <sup>131</sup>I: comparison of the results obtained in recurrent and newly diagnosed tumors [abstract]. *Cancer Res Suppl*. 1995;55:595.
9. Papanastassiou V, Pizer BL, Coakham HB, Bullimore J, Zananiri T, Kemshead JT. Treatment of recurrent and cystic malignant gliomas by a single intracavity injection of <sup>131</sup>I monoclonal antibody: feasibility, pharmacokinetics and dosimetry. *Br J Cancer*. 1993;67:144-151.
10. DeNardo GL, Maddock SW, Sgouros G, Scheibe PO, DeNardo SJ. Immunoadsorption: an enhancement strategy for radioimmunotherapy. *J Nucl Med*. 1993;34:1020-1027.
11. Goodwin DA. Tumor pretargeting: almost the bottom line. *J Nucl Med*. 1995;36:876-879.
12. Goodwin DA. Use of specific antibody for rapid clearance of circulating blood background from radiolabeled tumor imaging proteins. *Eur J Nucl Med*. 1984;9:209-215.
13. Hnatowich DJ, Virzi F, Ruskowski M. Investigations of avidin and biotin for imaging applications. *J Nucl Med*. 1987;28:1294-1302.
14. Green NM. Avidin and streptavidin. In: Wilchek, Bayer E, eds. *Methods of Enzymology: Avidin-Biotin Technology*. San Diego, CA: Academic Press; 1990:51-67.
15. Kalofonos HP, Ruskowski M, Siebecker DA, et al. Imaging of tumor in patients with In-111-labeled biotin and streptavidin-conjugated antibodies: preliminary communication. *J Nucl Med*. 1990;31:1791-1796.
16. Axworthy DB, Fritzberg AR, Hylarides MD, et al. Preclinical evaluation of an anti-tumor monoclonal/streptavidin conjugate for pretargeted <sup>90</sup>Y radioimmunotherapy in a mouse xenograft model [abstract]. *J Immunother*. 1994;16:158.
17. Axworthy DB, Theodore LJ, Gustavson LM, Reno JM, inventors; NeoRx Corp., assignee. Biotinidase resistance DOTA-biotin conjugates. US patent 5,608,060. March 4, 1997.
18. Wilchek M. Lectin-mediated isolation of cell surface glycoproteins. In: Wilchek M, Bayer E, eds. *Methods of Enzymology: Avidin-Biotin Technology*. San Diego, CA: Academic Press, 1990:306-314.
19. Stadalnik RC, Vera DR, Woodle S, et al. Technetium-99m NGA functional hepatic imaging: preliminary clinical experience. *J Nucl Med*. 1985;26:1233-1242.
20. Axworthy DB, Reno JM, inventors; NeoRx Corp., assignee. Hexose derived human serum albumin clearing. US patent 5,616,690. April 1, 1997.
21. Goodwin DA, Meares CF, Watanabe N, et al. Pharmacokinetics of pretargeted monoclonal antibody 2D12.5 and <sup>90</sup>Y-Janus-2(p-nitrobenzyl)-1,4,7,10-tetraazacyclododecane-tetraacetic acid (DOTA) in BALB/c mice with KHJ mouse adenocarcinoma: a model for radioimmunotherapy. *Cancer Res*. 1994;54:5937-5946.
22. Breitz HB, Tyler A, Bjorn MJ, Lesley T, Weiden PL. Clinical experience with <sup>99m</sup>Tc nofetumomab merpentan (Verluma) radioimmunoscintigraphy. *Clin Nucl Med*. 1997;22:615-620.
23. Breitz HB, Sullivan K, Nelp WB. Imaging lung cancer with radiolabeled antibodies. *Semin Nucl Med*. 1993;23:127-132.
24. Su F-M, Hickey JJ, Taylor C, Beaumier P. In-111/Y-90 dual isotope scintillation counting method for patient samples from pretargeted cancer therapy phase I trial [abstract]. *J Nucl Med*. 1996;3(suppl):145P.
25. Snyder WS, Ford MR, Warner GG. *Estimates of Specific Absorbed Fractions for Photon Sources Uniformly Distributed in Various Organs of a Heterogeneous Phantom*. MIRD Pamphlet No. 5. New York, NY: Society of Nuclear Medicine; 1978:5-67.
26. Loevinger R, Budinger TF, Watson EE. *MIRD Primer for Absorbed Dose Calculations*. New York, NY: Society of Nuclear Medicine; 1988.
27. International Commission on Radiation Units and Measures. Methods of assessment of absorbed dose in clinical use of radionuclides. In: International Commission on Radiation Units and Measurements. *ICRU Report 32*. Washington, DC: Department of Health, Education, and Welfare; 1979.
28. Fisher DR, Badger CC, Breitz HB, et al. Internal radiation dosimetry for clinical testing of radiolabeled monoclonal antibodies. *Antibod Immunconjug Radiopharm*. 1991;4:655-664.
29. Eve IS. A review of the physiology of the gastrointestinal tract in relation to radiation absorbed doses from radioactive materials. *Health Phys*. 1966;12:131-161.
30. Siegel JA, Wessels BW, Watson EE, et al. Bone marrow dosimetry and toxicity for radioimmunotherapy. *Antibod Immunconjug Radiopharm*. 1990;3:213-233.
31. Oken MM, Creech RH, Tormey DC, et al. Toxicity and response criteria for the Eastern Cooperative Group. *Am J Clin Oncol*. 1982;5:649-655.
32. Fritzberg AR. Antibody pretargeted radiotherapy: a new approach and a second chance. *J Nucl Med*. 1998;39:20N-22N.
33. Stickney DR, Slater JB, Kirk GA, et al. Bifunctional antibody: ZCE/CHA <sup>111</sup>indium BLEDTA-IV antibody 2D12.5 and <sup>90</sup>Y-Janus-2(p-nitrobenzyl)-1,4,7,10-tetraazacyclododecane-tetraacetic acid (DOTA) in BALB/c mice with KHJ mouse adenocarcinoma: a model for radioimmunotherapy. *Cancer Res*. 1994;54:5937-5946.
34. Le Doussal J-M, Martin M, Gautherot E, Delaage M, Barbet J. In vitro and in vivo targeting of radiolabeled monovalent and divalent haptens with dual specificity monoclonal antibody conjugates: enhanced divalent hapten affinity for cell-bound antibody conjugate. *J Nucl Med*. 1989;30:1358-1366.
35. Le Doussal J-M, Chetanneau A, Gruaz-Guyon A, et al. Bispecific monoclonal antibody mediated targeting of an indium-labeled DTPA dimer to primary colorectal tumors: pharmacokinetics, biodistribution, scintigraphy and immune response. *J Nucl Med*. 1993;34:1662-1671.
36. Vuillez JP, Moro D, Bodere F, et al. Radioimmunotherapy of small cell lung carcinoma with the two-step method using a bispecific anti-CEA/anti-DTPA antibody and the iodine-131 di-DTPA hapten: preliminary results. *J Nucl Med*. 1998;39P-70P.
37. Kraeber F, Bodere S, Bardet JP, et al. Phase I/II trial of two-step radioimmunotherapy in medullary thyroid cancer using bispecific anti-CEA/anti-DTPA-In antibody and I-131-labeled bivalent hapten [abstract]. *J Nucl Med*. 1998;39(suppl):246P.
38. Paganelli G, Magnani P, Zito F, et al. Three-step monoclonal antibody tumor targeting in carcinoembryonic antigen-positive patients. *Cancer Res*. 1991;51:5960-5966.
39. Paganelli G, Grana C, Cremenosi M, et al. Antibody guided therapy for high grade lymphoma with <sup>90</sup>Y-biotin [abstract]. *J Nucl Med*. 1998;39(suppl):70P.
40. Breitz H, Knox S, Weiden P, et al. Pretargeted radioimmunotherapy with antibody-streptavidin and Y-90 DOTA-biotin (avidin): results of a dose escalation study [abstract]. *J Nucl Med*. 1998;39(suppl):71P.